

See discussions, stats, and author profiles for this publication at: <https://www.researchgate.net/publication/249358004>

Thermo-Electro-Mechanical Performance of Piezoelectric Stack Actuators for Fuel Injector Applications

Article in *Journal of Intelligent Material Systems and Structures* · March 2009

DOI: 10.1177/1045389X08095030

CITATIONS

58

READS

703

5 authors, including:



M. S. Senousy

University of British Columbia - Vancouver

13 PUBLICATIONS 191 CITATIONS

SEE PROFILE



Faxin Li

Peking University

141 PUBLICATIONS 1,649 CITATIONS

SEE PROFILE



M. S. Gadala

University of British Columbia - Vancouver

145 PUBLICATIONS 2,398 CITATIONS

SEE PROFILE



Nimal Rajapakse

Simon Fraser University

230 PUBLICATIONS 5,534 CITATIONS

SEE PROFILE

Some of the authors of this publication are also working on these related projects:



Modelling of hydrogen diffusion in advanced material [View project](#)



piezoelectric [View project](#)

Journal of Intelligent Material Systems and Structures

<http://jim.sagepub.com>

Thermo-electro-mechanical Performance of Piezoelectric Stack Actuators for Fuel Injector Applications

M.S. Senousy, F.X. Li, D. Mumford, M. Gadala and R.K.N.D. Rajapakse

Journal of Intelligent Material Systems and Structures 2009; 20; 387 originally published online Sep 3, 2008;

DOI: 10.1177/1045389X08095030

The online version of this article can be found at:
<http://jim.sagepub.com/cgi/content/abstract/20/4/387>

Published by:



<http://www.sagepublications.com>

Additional services and information for *Journal of Intelligent Material Systems and Structures* can be found at:

Email Alerts: <http://jim.sagepub.com/cgi/alerts>

Subscriptions: <http://jim.sagepub.com/subscriptions>

Reprints: <http://www.sagepub.com/journalsReprints.nav>

Permissions: <http://www.sagepub.co.uk/journalsPermissions.nav>

Citations <http://jim.sagepub.com/cgi/content/refs/20/4/387>

Thermo-electro-mechanical Performance of Piezoelectric Stack Actuators for Fuel Injector Applications

M. S. SENOUSY,¹ F. X. LI,¹ D. MUMFORD,² M. GADALA¹ AND R. K. N. D. RAJAPAKSE^{1,*}

¹Department of Mechanical Engineering, University of British Columbia, Vancouver, BC, Canada V6T 1Z4

²Westport Innovations Inc., 101 - 1750 West 75th Ave., Vancouver, BC, Canada V6P 6G2

ABSTRACT: Piezoelectric actuators are increasingly used in fuel injectors due to their quick response, high efficiency, accuracy, and excellent repeatability. Current understanding of their thermo-electro-mechanical performance under dynamic driving conditions appropriate for fuel injection is, however, limited. In this paper, the thermo-electro-mechanical performance of soft Lead Zirconate Titanate (PZT) stack actuators is experimentally investigated over a temperature range of -30°C to 80°C , under driving electric fields of up to 2.0 kV/mm (using an AC drive method and a biased DC offset), different frequencies, and a constant preload of about 5 MPa . Experimental results show that the dynamic stroke of the actuators increases with the magnitude and frequency of the applied electric field, as well as ambient temperature. The dynamic stroke was also found to increase with decreased driving field rise time, which is equivalent to increasing the driving field frequency. At driving frequencies lower than the resonance frequency of the test apparatus ($\approx 500\text{ Hz}$), the strain-electric field behavior under different temperatures agreed well with previously obtained quasi-static results. The duty cycle was found to have a minimal effect on dynamic stroke but significantly affected the amount of heat generated under high electric field magnitudes and/or frequencies. The temperature increase due to self-heat generation under a continuous AC driving field (100% duty cycle) was very high, and limited the maximum driving field magnitude and/or frequency. Reducing the duty cycle significantly decreased the amount of heat generation.

Key Words: actuators, fuel injectors, piezoelectricity, stroke, temperature.

INTRODUCTION

PIEZOELECTRIC ceramic elements are used as distributed sensors and actuators in many engineering applications because of their direct and converse piezoelectric effects. Industrial piezoelectric devices are subject to high temperatures, thus must be designed to withstand thermal effects. These devices are also widely used in dynamically loaded systems that require fast, reliable, and precise actuation performance. Modern internal combustion engines are a cutting-edge example of such dynamic systems, where fuel injectors based on piezoelectric actuators are used to open and close fuel injection valves. A critical component of this new generation of fuel injectors is the piezoelectric stack actuator, which controls the injection process via an applied electric field. This actuator represents a promising improvement in direct fuel injection technology, with its precise positioning and rapid response time compared with conventional solenoid technology.

A multilayer piezoelectric actuator consists of piezoelectric thin discs with adjacent discs having opposite poling directions bonded together and sandwiched between electrodes. The axial length of a typical actuator used in fuel injectors can change by up to 0.12% by applying an electric field across the layer elements; the resultant actuator stroke can be calculated by multiplying the total number of layers by the net displacement of a single layer. This stroke is used to activate a valve needle that allows the fuel to be injected and controlled. Since the valve is actuated more quickly with piezoelectric actuators than with conventional solenoids, very precise injection intervals are possible between pre- and main injection, which significantly reduces emissions. Furthermore, piezoelectric actuator-based injectors allow an increase in the injection pressure, up to 250 MPa ; the higher the pressure and the more accurate the dosing and timing of the injection, the more efficient (and therefore less polluting) the combustion event becomes. Piezoelectric actuators in direct fuel injection have been shown to reduce fuel consumption in diesel and gas engines by up to 15% (Scharf, 2006). Overall, the advantages of piezoelectric injectors over conventional solenoid technology are that they provide an

*Author to whom correspondence should be addressed.
E-mail: rajapakse@mech.ubc.ca
Figures 2–19 appear in color online: <http://jim.sagepub.com>

optimized injection system (i.e., quieter, more economical, more powerful, reduced emissions (Boecking and Sugg, 2006)). It should be noted that whereas the needle stroke was fixed in the previous electromagnetic injection systems, in injectors where the piezoelectric actuator acts directly on the needle, the needle stroke can be varied by changing the magnitude of the applied electric field, enabling better control over the valve opening. Boecking and Sugg (2006) proposed an optimal piezoelectric injection actuator for combustion engines that overcomes the drawbacks of solenoid valves, with an innovative design that accounts for heat dissipation of the actuator.

Fuel metering in the combustion chamber is important for reducing the level of emissions generated during the combustion process, while minimizing fuel consumption. Many proposals have been made to provide fuel metering control for fuel injector systems, including systems that employ piezoelectric fuel injectors (Takase, 1999; Gromek and Shen, 2000). Fujii and Toyao (2006) presented a highly reliable piezoelectric actuator used in Toyota diesel engines with an injection interval as low as 0.1 ms.

It is clear that fuel injector technology utilizing piezoelectric actuators holds much promise. It is therefore important to examine the performance and reliability of piezoelectric actuators under conditions that simulate the actual operating conditions of a fuel injector. The static and dynamic performance of stacked piezoelectric actuators has received some attention in the past (Andersen et al., 2000a, b; Yao et al., 2000; Heinzmann et al., 2002; Ardelean et al., 2004; Li et al., 2008), as well as that of disk-stacked actuators (Sakai et al., 1992). The quasi-static thermo-electro-mechanical performance of cylindrical PZT actuators manufactured by Kinetic Ceramics Inc. was investigated by the current authors (Li et al., 2008) over a temperature range of -30°C to 125°C . Ardelean et al., (2004) experimentally investigated Noliac piezoelectric actuators, examining their quasi-static characteristics at 1 Hz, with an offset voltage of 75 V and different peak-to-peak voltages. The dynamic behavior of these actuators was also investigated for frequencies up to 3 Hz, showing the displacement–voltage hysteresis. Heinzmann et al., (2002) experimentally investigated co-fired PI piezoelectric actuators (18 mm length and $5 \times 5 \text{ mm}^2$ cross-section). They used a maximum driving voltage of 120 V (although some measurements were carried out at a higher voltage of 150 V), which corresponds to a maximum electric field magnitude of 2.0 kV/mm for an active layer thickness of 60 μm . The actuators' behavior was studied over an ambient temperature range of -40°C to 150°C ; results showed that stack capacitance is linearly dependent on temperature. At a frequency of 200 Hz and a temperature range of $0.8\text{--}75^{\circ}\text{C}$, displacement was found to not be dependent on temperature (i.e., for a

constant voltage, displacement is almost constant with temperature fluctuations, increasing $<10\%$ at the highest applied electric field).

In this paper, we conduct a comprehensive investigation of the dynamic thermo-electro-mechanical response of a typical set of piezoelectric stack actuators under different ambient temperatures, electric field magnitudes, duty cycles, frequencies, and rise times. The temperature increase due to heat generation under continuous AC driving fields (100% duty cycle) is also studied for different frequencies and electric field magnitudes.

EXPERIMENTAL PROCEDURE

Custom-made PZT multilayer stack actuators manufactured by Kinetic Ceramics Inc. (www.kineticceramics.com) were used in this study. The actuators are made from soft PZT ceramics with a coercive field E_c of 1.08 kV/mm, and have a Curie temperature above 360°C (Kinetic Ceramics Inc.). Soft PZT ceramics have a higher dielectric loss factor $\tan \delta$ than hard PZT ceramics, which promotes heat generation under large electric field magnitude and/or frequency, a higher piezoelectric coefficient d , and a lower coercive field (Lynch, 1996, 1994; Lynch et al., 2000). Piezoelectric materials with a higher piezoelectric coefficient (soft) are advantageous for actuator applications because they produce a greater strain than harder materials in response to an applied electric field. Soft PZT ceramics are also characterized by highly mobile domain walls whereas hard PZT ceramics restrain the domain wall response so that higher electric field magnitudes are required for the same effect to be observed. Table 1 shows the geometry and properties of the actuators used in this study.

The test stand (shown in Figure 1) was placed inside a thermal chamber (TestEquity Model 1007C) with a temperature feedback control of 0.1°C . The temperature of the actuator was measured through a Resistance Temperature Detector (RTD) attached to the surface of the actuator. In injector applications, the piezoactuators are subjected to a compressive preload for alignment and other design requirements. Li et al. (2008) found that a preload of 0–40 MPa has a negligible effect on the

Table 1. PZT stack actuator characteristics.

Actuator diameter (mm)	5
Actuator length (mm)	30
Layer thickness (mm)	0.5
Number of layers (stacks)	54
Capacitance (nF)	69
Maximum operating voltage (V)	1000
Maximum operating electric field (kV/mm)	2.0
Longitudinal piezoelectric coefficient d_{33} (pC/N)	370
Young's modulus Y_{33} (GPa)	48

static response of an actuator. The actuators were therefore subjected to a constant compressive preload of 5 MPa throughout the testing; the preload was applied using a soft spring (30 N/mm) fixed by a screw nut and measured using a force sensor placed between the shaft and the moving loading head, which was in direct contact with the actuator. The other end of the actuator was placed on a fixed plate, allowing the displacement to be measured using a linear variable displacement transducer (LVDT), with a resolution of 0.1 μm . Four different wave forms, sine wave and trapezoidal waves A, B, and C (Figure 2), were applied using an Agilent 33220 A signal generator with variable wave frequencies. The chosen wave forms were based on the potential design requirements of fuel injectors. A TREK piezo driver/power amplifier model PZD700 was used. Since the maximum allowed negative voltage applied to the stacks was -200 V (-20% of allowable full operating voltage), a DC bias voltage had to be applied to ensure that the negative voltage peak did not exceed -200 V (-0.4 kV/mm). The actuator was operated at full vendor-specified voltage with a bias field of $+300\text{ V}$, and an AC field of $+500/-500\text{ V}$. Although the DC offset was kept at -20% of the applied voltage, its effect on dynamic stroke was also examined. The measured displacement, temperature, and force signals were input into a data acquisition system and simultaneously monitored by a computer.

The test procedure consisted of the following steps: (1) aligning the piezoelectric actuator with the center of the shaft and the loading head; (2) preloading the actuator using a screw nut through a spring; (3) choosing the desired wave form, electric field magnitude, and frequency using the signal generator; (4) switching the power amplifier on and adjusting the DC offset; (5) firing the actuator; and (6) recording data.

The actuators used in the previous static study conducted by the authors (Li et al., 2008) could not be

used for dynamic testing in this study as they are incompatible with the current driver; their high capacitance reduces the applied voltage at the actuator to about one-third of the commanded voltage. This difference in voltage is caused primarily by the reactive impedance of the piezoelectric actuators, which places some special requirements on the amplifier. In other words, the amplifier has to handle significantly higher voltages and circulating currents than are suggested by the real electrical/mechanical power requirements of the actuator. Additionally, Linder et al. (2001) showed that the electrical power at the actuator terminals has a negative real component, indicating that the actuator feeds electrical power back to the source. Since the current actuators are smaller and have lower capacitance than those used by Li et al. (2008), there is almost no difference between the two voltages.

In the current study, different controlling parameters were employed to obtain a better understanding of

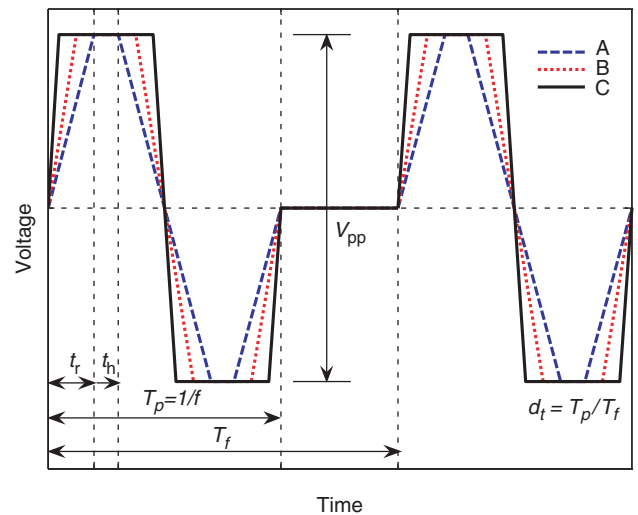


Figure 2. Illustration of the three different driving field trapezoidal waves (A, B, and C).

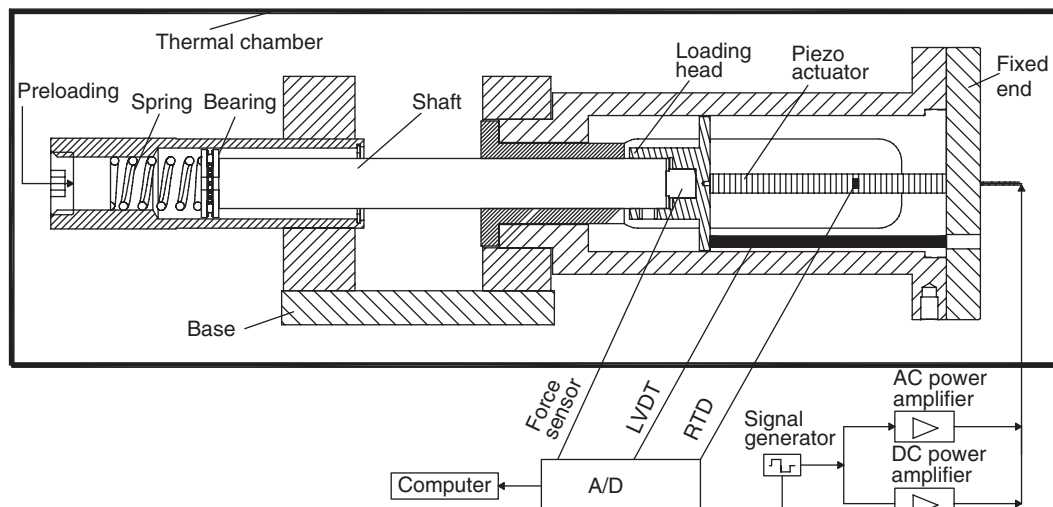


Figure 1. Test setup.

the dynamic behavior of the stacks. These parameters include the electric field magnitude E ($E = V_{pp}/h$, where V_{pp} is the applied peak-to-peak voltage and h is the thickness of a single layer), frequency f , driving field rise time t_r , biased DC offset voltage V_{dc} , duty cycle d_t , and ambient temperature. In addition, a sinusoidal wave form and three different trapezoidal waves A, B, and C with different rise times were used. Wave A had the longest rise time, $t_r = 0.2T_p$, where T_p is the driving field period, and C had the shortest rise time, $t_r = 0.05T_p$ (Figure 2). Holding time t_h is defined as the period over which a signal is kept constant at a peak value, $T_p = 4t_r + 2t_h$. Duty cycle is defined as the ratio between the driving field period and the period of a complete voltage cycle, T_f (i.e., $d_t = T_p/T_f$). A duty cycle of 100% means a continuous wave, while a 0% duty cycle implies no signal, or a DC signal.

EXPERIMENTAL RESULTS

Figure 3 shows the frequency dependence of the dynamic stroke under sinusoidal electric driving fields of 0.6, 1.0, and 1.5 kV/mm and a duty cycle of 10%. It can be seen from Figure 3 that below a frequency of 100 Hz, the dynamic stroke was almost constant. However, for frequencies higher than 100 Hz, the dynamic stroke increased almost linearly with the driving field frequency. It can also be seen that the rate of change of the stroke increased with increasing electric field magnitude as a result of the increased activities of non-180° domain walls at high electric field magnitudes (i.e., \geq coercive electric field). The resonance frequency, f_r , of the testing system (including the actuator, loading shaft, spring for preloading, etc.) was found to be about 511 Hz. This estimate is based on an actuator axial stiffness of 31 N/ μ m, a mass of 5 g, and a moving parts mass of 3 kg. Thus, as expected, when the driving field frequency

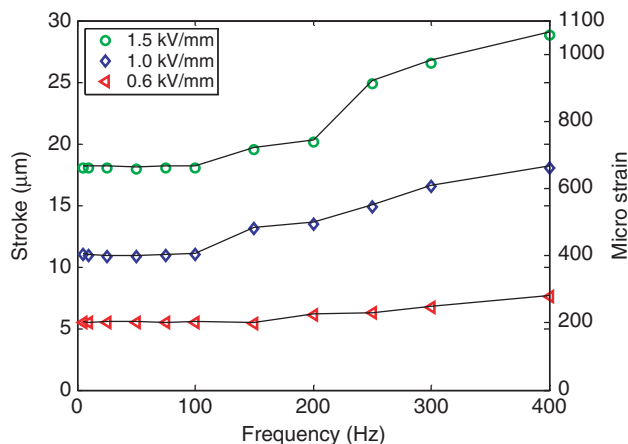


Figure 3. Variation of the dynamic stroke of piezoelectric stack actuators with driving frequency (sine wave and 10% duty cycle).

approached f_r , the dynamic stroke and system oscillations rapidly increased with frequency, as shown in Figure 4. Figure 5 shows the dynamic stroke for the four waveforms at a frequency of 100 Hz, a driving field magnitude of 1.0 kV/mm, and a 10% duty cycle. For all the driving waveforms considered, the dynamic stroke showed a highest ringing level at the trapezoidal wave C, which had the shortest rise time (Figure 5(d)). The decrease in rise time is believed to increase the effect of the sub-harmonics of the driving field, which may explain the increase in dynamic stroke ringing with decreased rise time.

Figure 6 shows the effect of duty cycle on dynamic stroke for the four different waveforms at $E = 1.0$ kV/mm and for different frequencies up to 300 Hz. It can be seen from the figure that the duty cycle had almost no effect on dynamic stroke for both sinusoidal and trapezoidal loading. Although duty cycle did not affect dynamic stroke, it strongly affected the temperature increase of the PZT actuators being considered in this study, except at low frequencies and electric field magnitudes. The duty cycle was therefore fixed at 10% in all remaining dynamic testing, except for the self-heat generation tests presented in the last section of this paper, where duty cycles up to 100% were investigated. Figure 6 also shows that the dynamic strokes corresponding to the three trapezoidal waves were larger than those corresponding to the sinusoidal wave. Furthermore, under trapezoidal loading, the shortest rise time yielded the largest stroke.

In Figure 7, dynamic stroke is plotted against rise time for different trapezoidal driving field magnitudes, with duty cycle constant at 10%. Dynamic stroke was found to increase with decreased driving field rise time. The rise-time dependence may be explained by the time dependence of the extrinsic response of PZT. Sherritt et al. (1992) reported that non-180° domain switching is time dependent and needs a finite time to occur, and that only domain wall motions that have sufficient time to occur contribute to the piezoelectric response. This result suggests that as rise time decreased in the current study (i.e., holding time increased), more domain walls may have had enough time to realign, causing a larger actuator stroke. The increasing effect of the sub-harmonics of the driving field may also explain the increase in stroke with decreased rise time. System inertia is also expected to have contributed to this response. In the practical case of a piezoelectric actuator in a fuel injector, the mass of the moving parts is much less than in the test stand. Therefore, the rise-time effect may differ in practices, but it will still show the decaying trend depicted in Figure 7.

Figure 8 shows the dependence of dynamic stroke on ambient temperature under a sinusoidal electric driving field with magnitude ranging from 0.6 to 2.0 kV/mm, a frequency of 100 Hz, and a duty cycle of 10%. It can be seen that dynamic stroke increased steadily with ambient

temperature under the range of driving field magnitudes considered. However, at driving fields of 1.0 kV/mm and above, a non-linear transition zone occurred between 40°C and 55°C, leading to an almost bilinear stroke–temperature curve. As discussed by Strukov and Levanyuk (1998), if domain wall density is in equilibrium state, new domain walls are not generated immediately after heating. Instead, a certain degree of heating is required for domain wall density to change noticeably and reach another equilibrium state. Accordingly, the non-linear transition zone observed in Figure 8 may be explained by the extrinsic contribution from increased domain wall density and non-180° domain switching-induced strain. The general trend of the dynamic stroke results shown in Figure 8 is similar to that found in static-stroke tests (Li et al., 2008), where a non-linear transition zone was observed between 25°C and 60°C.

To reveal the relationship between driving field magnitude and dynamic stroke over the desired ambient temperature range (−30°C to 80°C), Figure 8 is re-plotted in Figure 9. As expected, dynamic stroke increased with driving field magnitude, such that the stroke–electric field curves can be approximated by a bilinear curve with a slope modulation point at 0.6 kV/mm, and the slopes of the curves increase with ambient temperature. Li et al. (2008) found that in the static case, the static strain at the maximum driving field magnitude (1.8 kV/mm) was about 1.7 times the product of the electric field and the piezoelectric constant, d_{33} ,

measured at a low driving field. For the actuators used in this study, the dynamic strain at maximum driving field magnitude (2.0 kV/mm) was almost 1.6 times the product of the electric field and the piezoelectric constant, d_{33} , measured at a low driving field magnitude, which indicates that under higher driving field magnitudes, non-180° domain switching-induced strain may contribute to the piezoelectric response.

Assuming that the thermal-expansion coefficient α does not change with electric field magnitude, the longitudinal piezoelectric constant d_{33} at different temperatures can be calculated by dividing the induced longitudinal strain, indirectly measured using the LVDT, by the applied electric field. The d_{33} was calculated over a temperature range of −30°C to 80°C and electric field magnitudes of up to 2.8 kV/mm using the measured stroke. As expected, the longitudinal piezoelectric constant showed a non-linear dependence on electric field magnitude under different temperatures, as depicted in Figure 10, which is in good agreement with the results obtained at room temperature by Masys et al. (2003). For low electric field magnitudes (≤ 0.6 kV/mm), the material behavior was approximately linear and d_{33} was almost constant (Figure 10, region I). When the applied electric field increased, d_{33} increased non-linearly with E (Figure 10, region II). Figure 10 also shows that d_{33} increased with ambient temperature. The computed d_{33} of the stack actuator at room temperature and low driving fields was about 350×10^{-12} C/N,

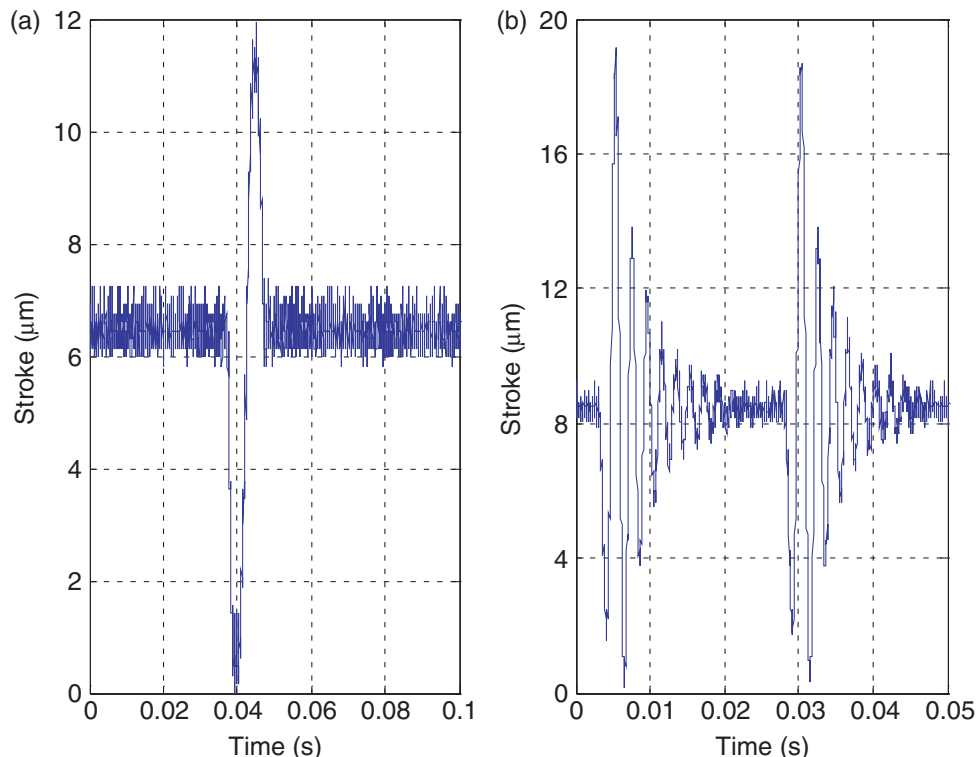


Figure 4. Dynamic stroke under (a) 100 Hz and (b) 400 Hz sinusoidal waveforms ($E = 1.0$ kV/mm and 10% duty cycle).

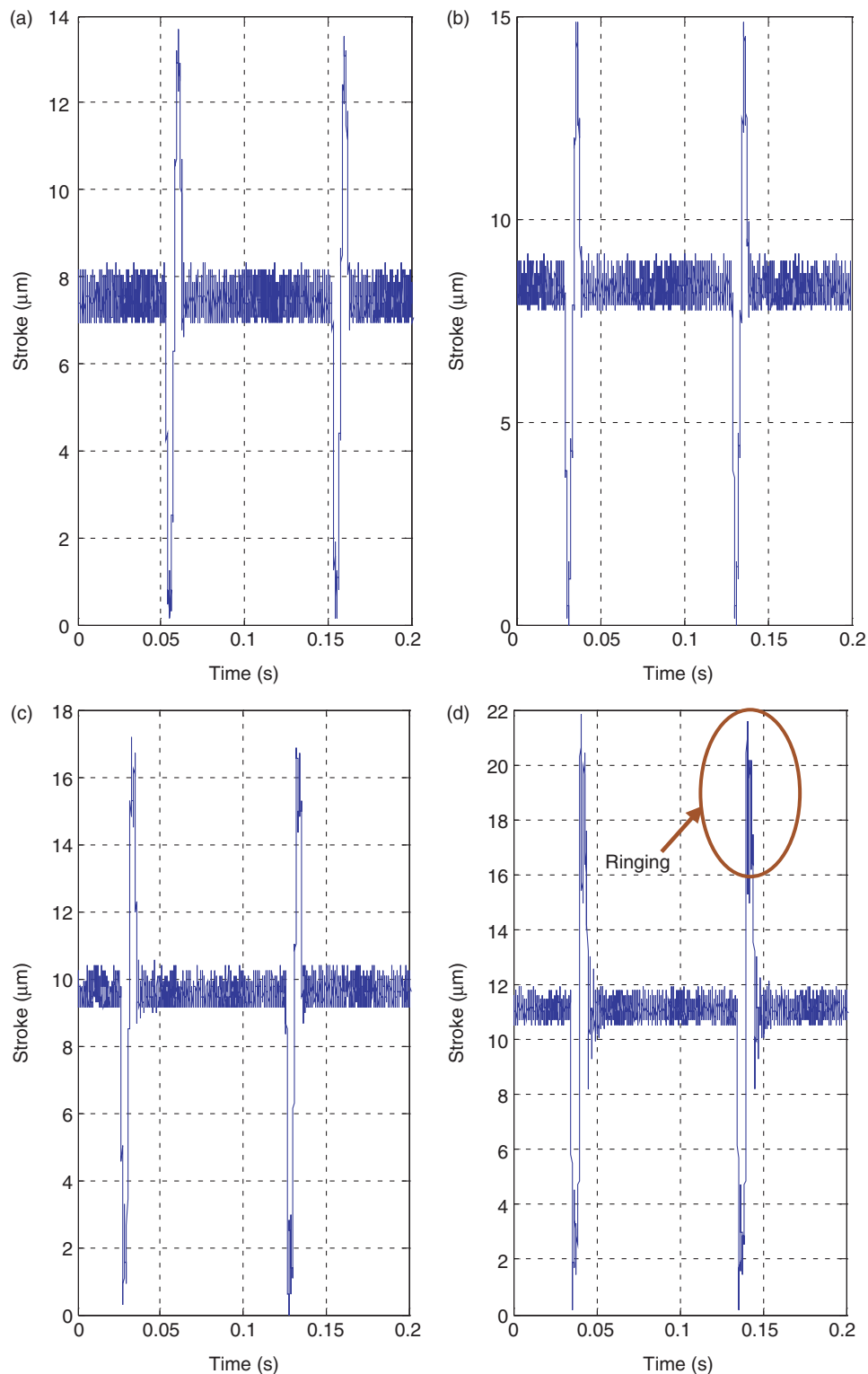


Figure 5. Dynamic stroke under (a) sine wave, (b) trapezoidal wave A, (c) trapezoidal wave B, and (d) trapezoidal wave C ($E = 1.0 \text{ kV/mm}$, $f = 100 \text{ Hz}$ and 10% duty cycle).

which is close to the vendor-specified data of $370 \times 10^{-12} \text{ C/N}$. At room temperature and an electric field magnitude of 2.0 kV/mm , d_{33} reached a value of $\approx 540 \times 10^{-12} \text{ C/N}$ ($\approx 55\%$ increase from the value at low driving field). In the temperature range -30°C to 80°C at low

electric field magnitudes, d_{33} increased by 125%. Zhang et al. (1994) stated that the change in piezoelectric coefficients with temperature is due to intrinsic and extrinsic contributions, with intrinsic piezoelectric contributions of less than 37% at room temperature.

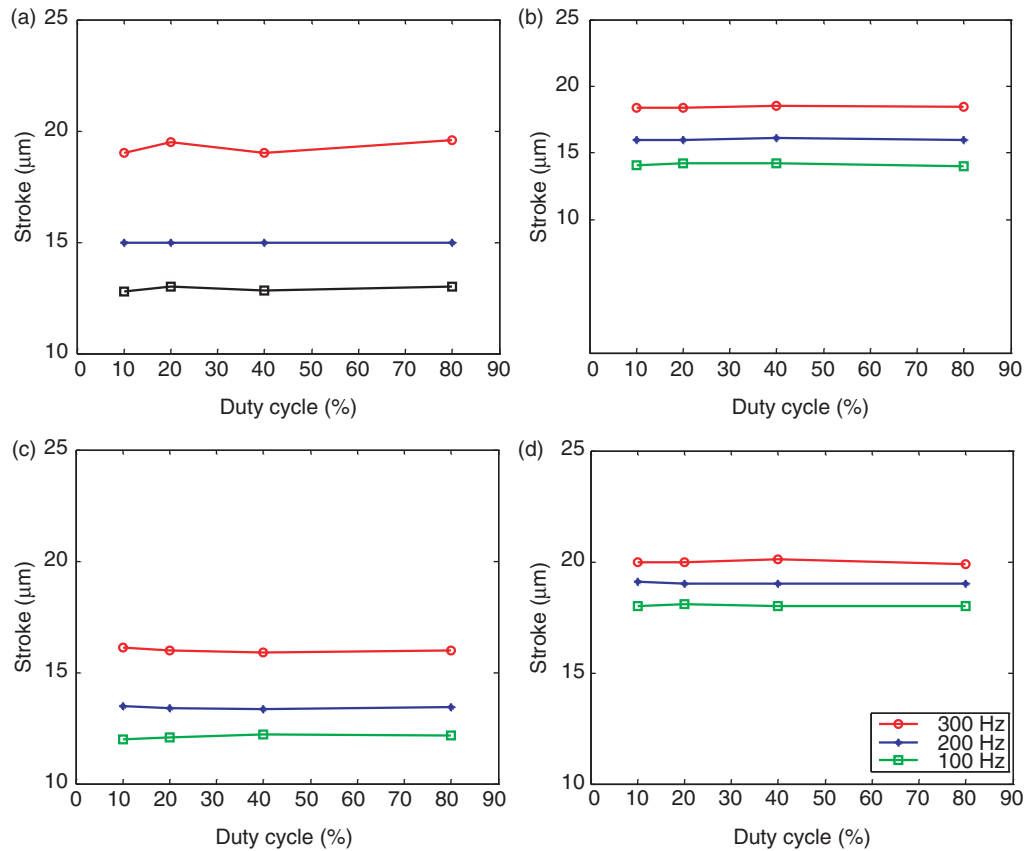


Figure 6. Effect of duty cycle on stroke for four different waveforms at $E = 1.0 \text{ kV/mm}$: (a) sine wave, (b) trapezoidal wave A, (c) trapezoidal wave B, (d) trapezoidal wave C.

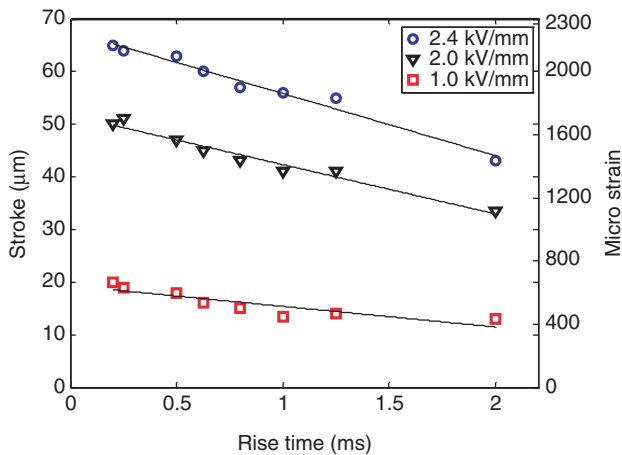


Figure 7. Effect of rise time on dynamic stroke for different trapezoidal driving field magnitudes at 10% duty cycle.

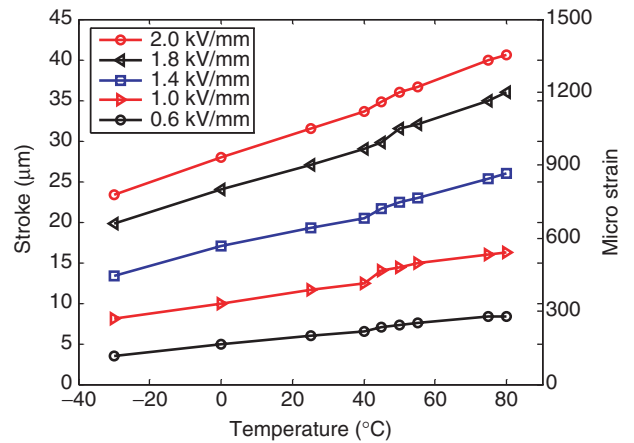


Figure 8. Variation of dynamic stroke with ambient temperature under different sinusoidal driving field magnitudes (100 Hz and 10% duty cycle).

Intrinsic properties are material properties from a single-domain material, while extrinsic properties are mainly from domain walls. They also stated that the extrinsic piezoelectric contributions increased rapidly with temperature as a result of non- 180° domain walls. Therefore, it can be concluded that for the actuator being considered in this study, at low driving field magnitudes $\leq 0.6 \text{ kV/mm}$ (Figure 11, region I), the linear change of

the piezoelectric coefficient with ambient temperature was mainly caused by extrinsic contributions due to domain walls, which were driven by temperature. At higher electric field magnitudes (Figure 11, region II), an additional extrinsic part was introduced to account for the increased activities of non- 180° domain walls caused by high electric field magnitudes (Li et al., 2008). Figure 11 is a re-plotting of Figure 10 to delineate the

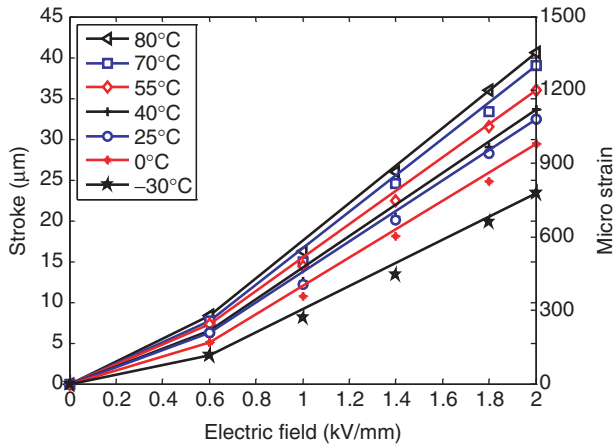


Figure 9. Variation of dynamic stroke with driving field magnitudes over an ambient temperature range of -30°C to 80°C (sinusoidal wave at 100 Hz and 10% duty cycle).

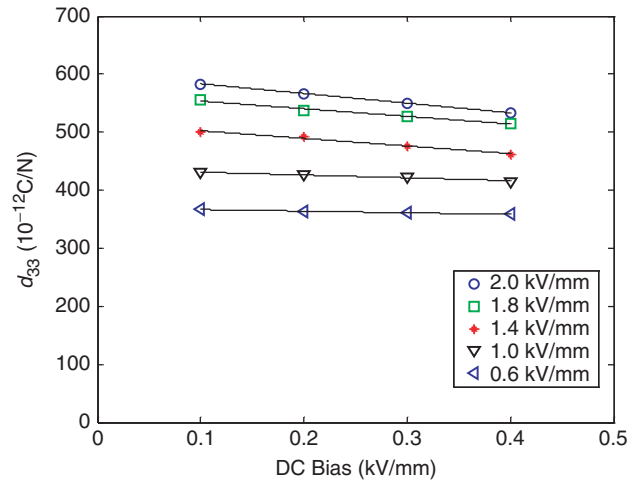


Figure 12. Variation of piezoelectric coefficient d_{33} with DC offset under different sinusoidal driving field magnitudes at room temperature (100 Hz and 10% duty cycle).

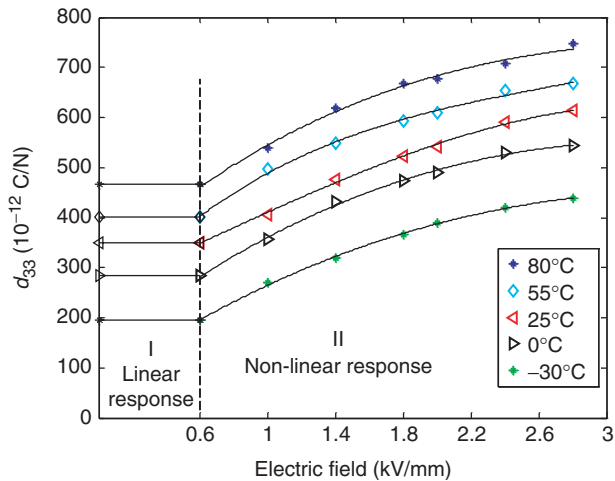


Figure 10. Variation of piezoelectric coefficient d_{33} with electric field magnitude (100 Hz and 10% duty cycle).

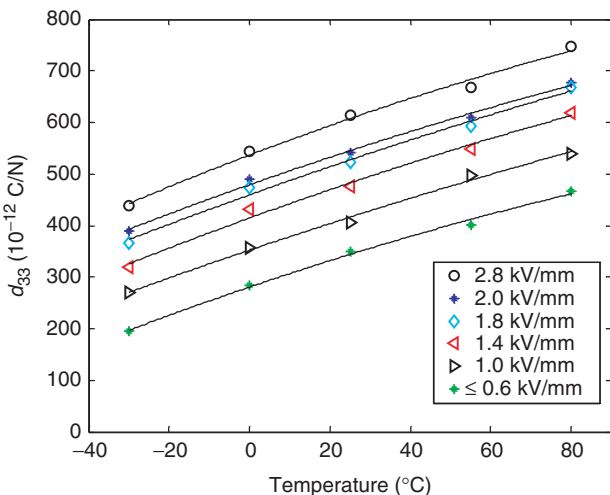


Figure 11. Variation of piezoelectric coefficient d_{33} with ambient temperature (100 Hz and 10% duty cycle).

variation of d_{33} with ambient temperature, and shows that d_{33} was linearly dependent on temperature, which is in good agreement with the results obtained by Zhang et al. (1994, 1995).

The effect on the longitudinal piezoelectric coefficient of changing DC offset was also investigated by applying different DC positive bias voltages. Figure 12 shows the biased DC offset dependence found of d_{33} under a sinusoidal peak-to-peak electric field magnitude ranging from 0.6 to 2.0 kV/mm, a frequency of 100 Hz, and a duty cycle of 10% at room temperature. For low electric field magnitudes <1.0 kV/mm, the DC offset was found to have almost no effect on d_{33} . At driving field magnitudes of 1.0 kV/mm and above, the longitudinal piezoelectric coefficient decreased slightly with the positive DC offset, which is in good agreement with the results obtained by Masys et al. (2003). Masys et al. (2003) reported that a positive bias field does not increase the total polarization, but does contribute to pinning of the domain walls, and hence reduces the extrinsic contribution to the piezoelectric response.

Heat Generation and Hysteresis in Actuators

Heat generation in PZT actuators was also investigated, since it was observed that a significant amount of heat is generated when PZT actuators are driven under high frequency and/or high electric field magnitudes. Heat generation can significantly affect the reliability and piezoelectric properties of these actuators, and may also limit their application. Heat generation in multi-layer PZT actuators is considered to be caused by losses, such as mechanical loss and dielectric loss (Ochi et al., 1985). However, it has been assumed in the literature to date that the major contribution to heat generation is from dielectric loss which is caused by ferroelectric

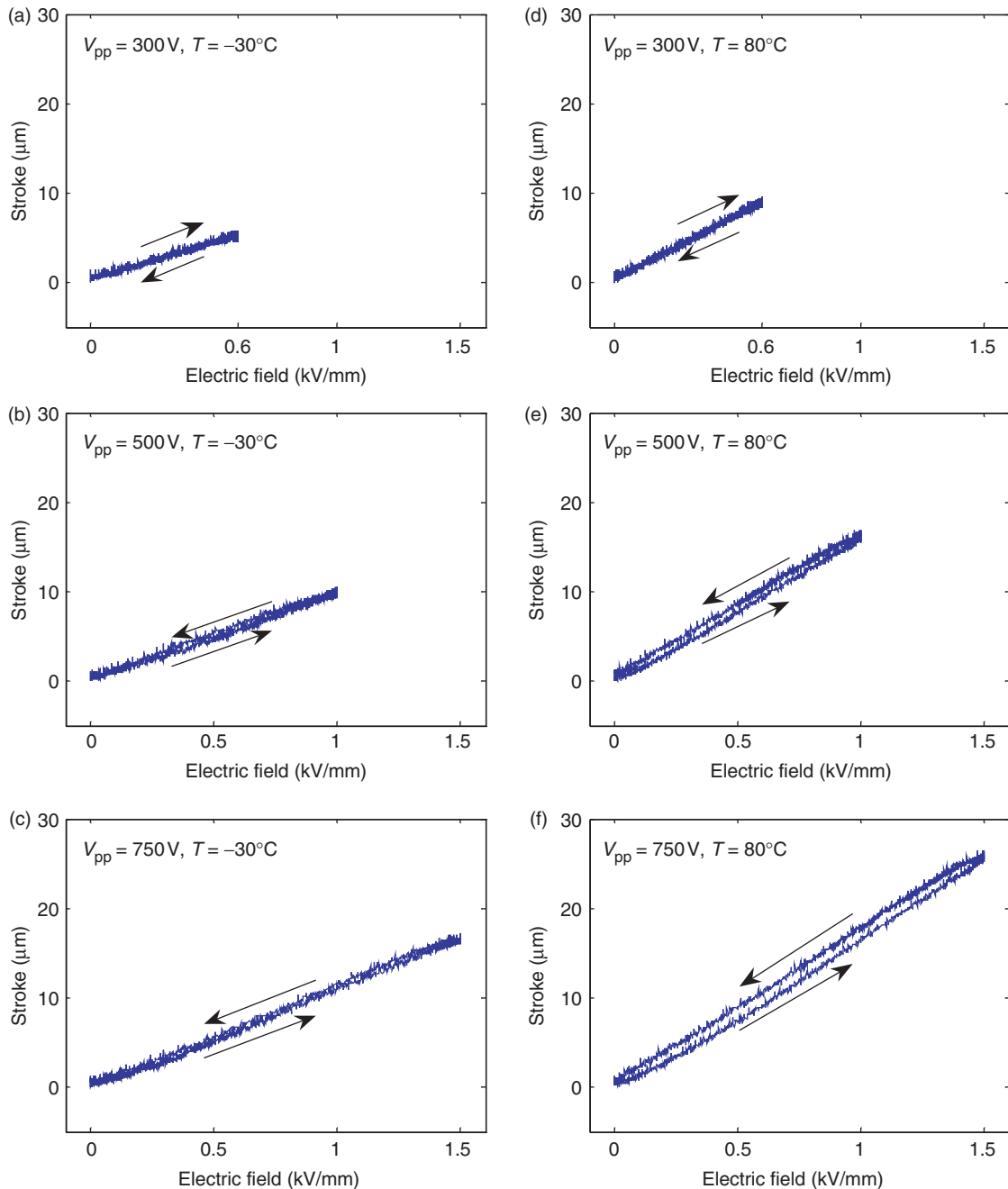


Figure 13. Effect of electric field magnitude on piezoelectric hysteresis at two different temperatures: (a–c) -30°C , (d–f) 80°C (sinusoidal wave form at 1Hz).

hysteresis loss (Zheng et al., 1996; Lesieutre et al., 1996; Uchino and Hirose, 2001).

The effect of the electric field magnitude and of ambient temperature on piezoelectric hysteresis is shown in Figure 13(a–c) and (d–f), at temperatures of -30 and 80°C , respectively, and a driving frequency of 1 Hz using a sinusoidal wave form. At electric field magnitudes $<0.6\text{ kV/mm}$, there was almost no hysteresis at both temperatures. On the other hand, for higher electric field magnitudes, hysteresis increased due to increased activities of non- 180° domain walls with increasing

temperature and electric field magnitude. As mentioned by Zhang et al. (1995), mathematical modeling of hysteresis and irreversible behavior in ferroelectric materials is rather complicated. According to them and Masys et al. (2003), most of the observed non-linearities and hysteresis in the material response are due to extrinsic contributions from the domain-boundary motion and phase-boundary motion.

For the purpose of heat generation testing in the current study, a 10min continuous loading cycle was used. The temperature increase of the selected actuators

under a continuous sinusoidal AC driving field (i.e., 100% duty cycle) is shown in Figure 14 for different frequencies up to 300 Hz, and different electric field magnitudes (0.6, 1.0, and 1.4 kV/mm). All tests were conducted at room temperature, with 25°C as the

reference temperature T_0 (ambient temperature inside the chamber). The temperature increase, δT , is defined as $(\delta T = T_i - T_0)$, where T_i is the measured temperature of the actuator surface.

It can be seen from Figure 14 that self-heat generation in the PZT actuators tested increased with increasing electric field magnitude and frequency. The temperature increase in actuators showed an initially increasing trend and then reached a steady state temperature. The time at which the steady state was achieved, as well as the value of the steady state temperature, was governed by the electric field magnitude and frequency. For instance, for $E = 1.4$ kV/mm and $f = 300$ Hz, the steady state temperature was almost 60°C, while for $E = 0.6$ kV/mm and $f = 100$ Hz, the steady state temperature was close to 1.5°C. Since the dynamic stroke was found to be dependent on ambient temperature, one can expect the dynamic stroke to increase with time as the actuator temperature increases, as shown in Figure 15. Note that the increase in stroke here is due to self-heat generation which increases the extrinsic piezoelectric contribution, non-180° domain switching-induced strain (Figure 8).

The variation of the steady state temperature increase δT_∞ with frequency is shown in Figure 16 for different driving electric field magnitudes and a 100% duty cycle. For driving field magnitudes < 0.6 kV/mm, the steady state temperature increase was linearly proportional to the driving field frequency. However, as the magnitude of the electric field increased, the temperature–frequency relation was no longer linear. A power law fit using the least-squares technique was used to depict the steady state temperature–frequency relation such that $\delta T_\infty = af^b$ (where, a and b are functions of the applied electric field, and $b \geq 1.0$).

Self-heat generation in piezoelectric actuators was also found to depend on electric field magnitude. Figure 17 shows the dependence of the steady state temperature

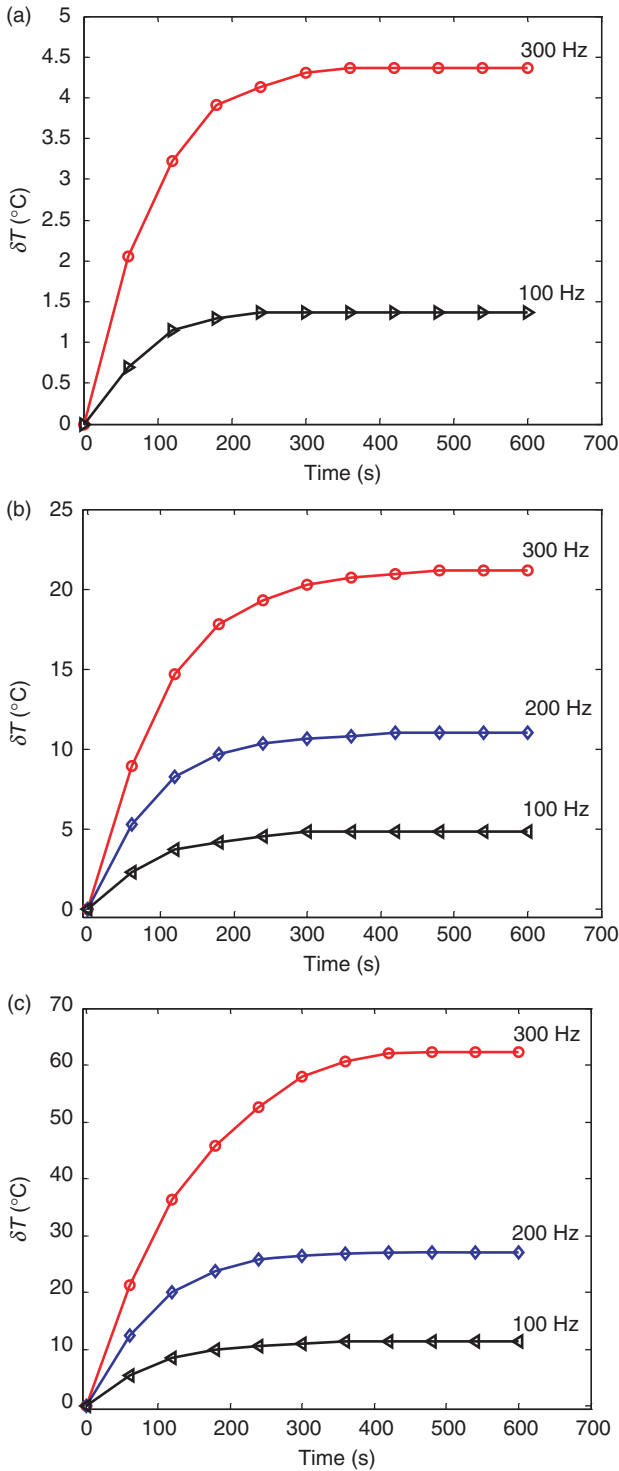


Figure 14. Temperature increase with time under different frequencies and continuous sinusoidal electric fields: (a) 0.6 kV/mm, (b) 1.0 kV/mm, and (c) 1.4 kV/mm.

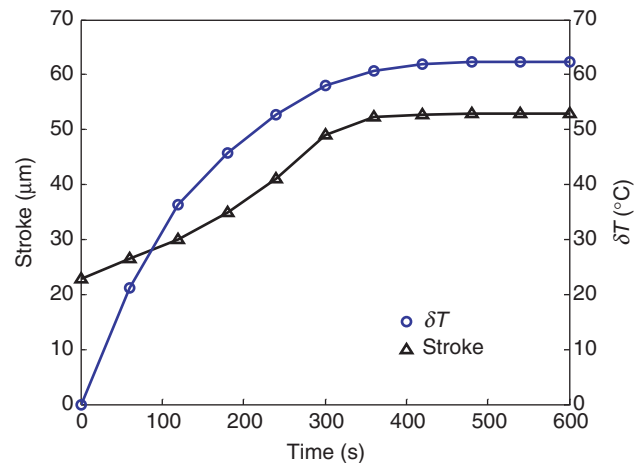


Figure 15. Variation of dynamic stroke with time under dynamic driving conditions ($E = 1.4$ kV/mm, $f = 300$ Hz, and 100% duty cycle).

increase of the actuators tested on electric field magnitude. For driving field frequencies <100 Hz, the steady state temperature increase was almost linearly proportional to the electric field magnitude. As the frequency increased (≥ 100 Hz), a non-linear trend was observed with δT_{∞} being almost proportional to E^3 .

Although duty cycle did not affect the dynamic stroke, it significantly affected self-heat generation under dynamic operating conditions. For example, doubling the duty cycle nearly doubled the steady state temperature increase. Figure 18 shows the dependence of the temperature increase on duty cycle for different loading frequencies at $E = 1.4$ kV/mm. Steady state temperature increase in piezoelectric actuators was found to be linearly dependent on duty cycle, as shown in Figure 19. Decreasing duty cycle significantly decreased

the heat generated in the piezoelectric actuators tested. Thus decreasing the duty cycle can improve the functionality of these actuators and lead to their expanded use in high-power applications.

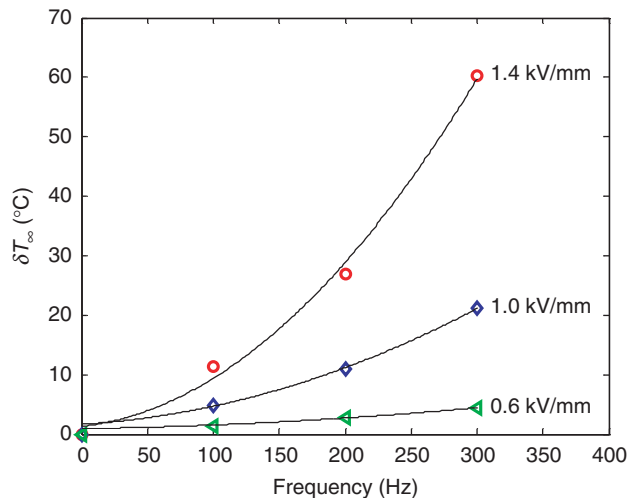


Figure 16. Variation of steady state temperature increase with frequency for different electric field magnitudes.

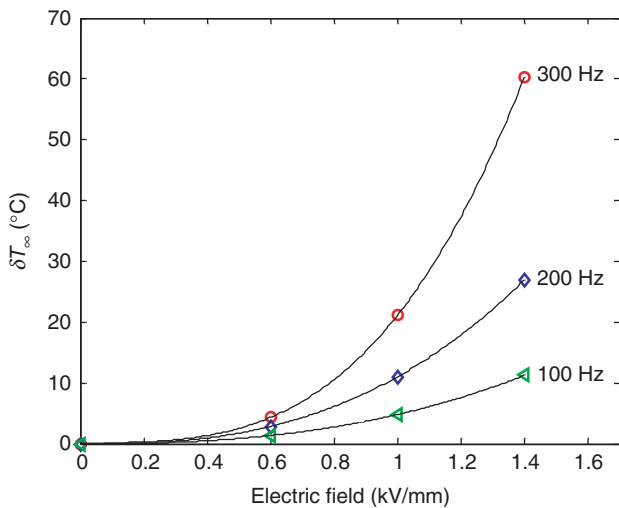


Figure 17. Variation of steady state temperature increase with electric field magnitude for different frequencies.

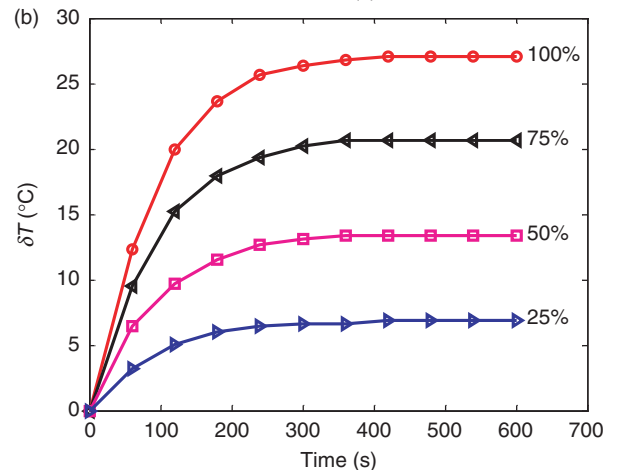
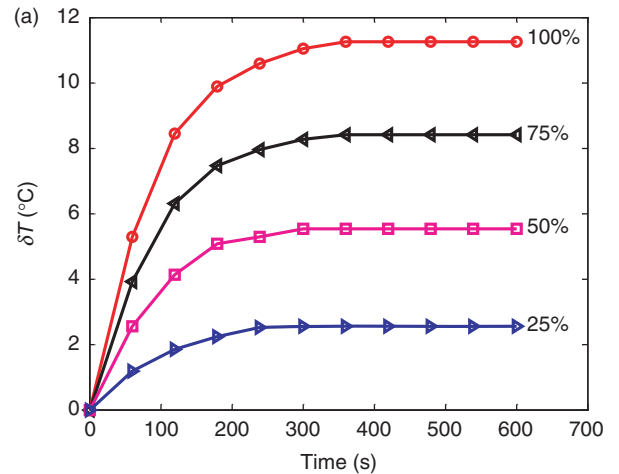


Figure 18. Variation of temperature increase with time for different duty cycles under two different frequencies ($E = 1.4$ kV/mm): (a) 100 Hz, (b) 200 Hz.

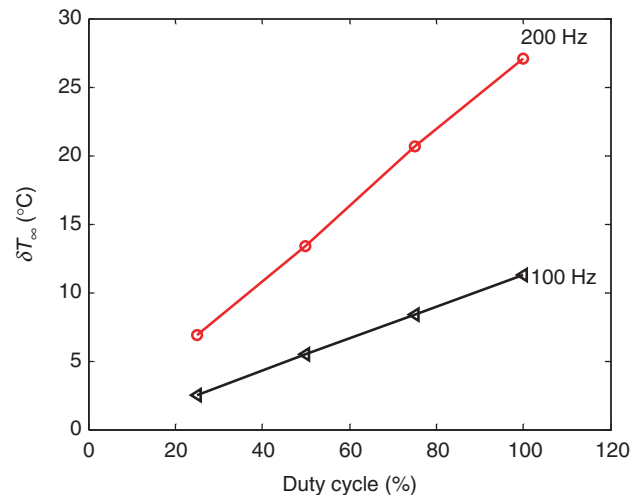


Figure 19. Dependence of steady state temperature increase on duty cycle percentage ($E = 1.4$ kV/mm).

Zheng et al. (1996) proposed a theoretical model to explain the mechanism of heating in piezoelectric materials. The model was based on the law of energy conservation, and the assumption that the rate of heat generation is directly proportional to the frequency and hysteresis loss per driving cycle per unit volume. Polarization-electric field hysteresis was found to be approximately proportional to E^2 and linearly proportional to frequency f . The mathematical model represents a closed-form solution for temperature increase that shows the classical exponential variation with respect to time, as well as a steady state value. However, since the dependence of hysteresis on duty cycle and ambient temperature was not considered in the model, it cannot be used to simulate the results of Figures 14–18. The authors are currently formulating a mathematical model that accounts for the effects of duty cycle, as well as the dependency of piezoelectric losses on ambient temperature, electric field magnitude, and frequency.

CONCLUSION

The thermo-electro-mechanical performance of piezoelectric stack actuators under different operating conditions relevant to fuel injection was investigated in this paper. Soft epoxy-bonded PZT stack actuators were tested over a temperature range of -30°C to 80°C , under sinusoidal and trapezoidal driving fields of up to 2.0 kV/mm with various frequencies, rise times, and duty cycles. The effect of the biased DC offset voltage on the dynamic performance of PZT stacks was also studied. The biased DC offset was found to slightly affect the dynamic stroke of PZT actuators by reducing the extrinsic contribution due to non- 180° domain walls. Below the resonance frequency of the testing system (about 511 Hz), the dynamic stroke was found to increase with driving field frequency. In the case of the trapezoidal loading field, a decrease in rise time increased the non- 180° domain wall motions; decreasing the rise time was found to be equivalent to increasing the frequency (i.e., dynamic stroke increased with decreasing rise time). Self-heat generation in the actuators was also investigated for different combinations of electric field magnitude, frequency, and duty cycle. Heat generation increased with increased driving field magnitude and driving field frequency. Although duty cycle had almost no effect on dynamic stroke, it strongly affected heat generation in the actuators. Decreasing the duty cycle can significantly decrease heat generated in the actuators. At driving field frequencies much lower than the resonance frequency of the system, the stroke-electric field behavior at different temperatures agreed well with the quasi-static results obtained previously.

ACKNOWLEDGMENT

The authors are grateful to Damien Clapa, Charlie Loo, and Liam Segarty of Westport Power Inc. for providing assistance during testing. This research was supported by a grant from the Natural Sciences and Engineering Research Council (NSERC) of Canada with substantial in-kind support provided by Westport Power Inc.

REFERENCES

- Andersen, B., Ringgaard, E., Bove, T., Albareda, A. and Pérez, R. 2000a. "Performance of Piezoelectric Ceramic Multilayer Components Based on Hard and Soft PZT," In: *Actuator 2000: Seventh International Conference on New Actuators*, pp. 419–422.
- Andersen, B., Ringgaard, E. and Nielsen, L.S. 2000b. "Static and Dynamic Performance of Stacked Multilayer Actuators Based on Hard and Soft PZT," In: *Actuator 2000: Seventh International Conference on New Actuators*, pp. 423–426.
- Ardelean, E.V., Cole, G.D. and Clark, R.L. 2004. "High Performance 'V-Stack' Piezoelectric Actuator," *Journal of Intelligent Material Systems and Structures*, 15:879–899.
- Boecking, F. and Sugg, B. 2006. "Piezo Actuators: A Technology Prevails with Injection Valves for Combustion Engines," In: *Actuator 2006: Tenth International Conference on New Actuators*, pp. 171–176.
- Fujii, A. and Toyao, T. 2006. "Piezoelectric Actuators with High Reliability for Diesel Injection Valve," In: *Actuator 2006: Tenth International Conference on New Actuators*, pp. 177–180.
- Gromek, B. and Shen, J.J. 2000. "Multiple Stack Piezoelectric Actuators for a Fuel Injector," United States Patent, Patent Number 6-345-771 B1.
- Heinzmann, A., Hennig, E., Kolle, B., Kopsch, D., Richter, S., Schwotzer, H. and Wehrsdorfer, E. 2002. "Properties of PZT Multilayer Actuators," In: *Actuator 2002: Eighth International Conference on New Actuators*, P03.
- Kinetic Ceramics Inc. (<http://www.kineticceramics.com>).
- Lesieutre, G.A., Fang, L., Koopmann, G.H., Pai, S.P. and Yoshikawa, S. 1996. "Heat Generation of a Piezoceramic Induced Strain Actuator Embedded in a Glass/epoxy Composite Panel," *Proceedings of SPIE – The International Society for Optical Engineering*, 2717:267–275.
- Li, F.X., Rajapakse, R.K.N.D., Mumford, D. and Gadala, M. 2008. "Quasi-static Thermo-electro-mechanical Behaviour of Piezoelectric Stack Actuators," *Smart Materials and Structures*, 17:015049.
- Linder, D.K., Vujic, N. and Leo, D.J. 2001. "Comparison of Drive Amplifier for Piezoelectric Actuators," *Proceedings of SPIE – The International Society for Optical Engineering*, 4332:281–291.
- Lynch, C.S. 1994. "Electro-mechanical Coupling in 8/65/35 PLZT," In: *Proceedings of the Ninth IEEE International Symposium*, pp. 357–360.
- Lynch, C.S. 1996. "The Effect of Uniaxial Stress on the Electro-Mechanical Response of 8/65/35 PLZT," *Acta Materialia*, 44(10):4137–4148.
- Lynch, C.S., Chen, W. and Liu, T. 2000. "Multiaxial Constitutive Behavior of Ferroelectric Materials," *Proceedings of SPIE – The International Society for Optical Engineering*, 3992:245–254.
- Masys, A.J., Ren, W., Yang, G. and Mukherjee, B.K. 2003. "Piezoelectric Strain in Lead Zirconate Titanate Ceramics as a

- Function of Electric Field, Frequency and DC Bias," *Journal of Applied Physics*, 94(2):1155–1162.
- Ochi, A., Takahashi, S. and Tagami, S. 1985. "Temperature Characteristics for Multilayer Piezoelectric Ceramic Actuators," *Japanese Journal of Applied Physics*, 24(Suppl. 24-3):209–212.
- Sakai, T., Ishikiryama, M. and Shimazaki, R. 1992. "Durability of Piezoelectric Ceramics for an Actuator," *Japanese Journal of Applied Physics*, 31:3051–3054.
- Scharf, A. 2006. "Prize-winning Piezo," Piezo-actuators in Fuel Injection Systems, EPCOS technical articles, (www.epcos.com).
- Sherrit, S., Van Nice, D.B., Graham, J.T., Mukherjee, B.K. and Wiederick, H.D. 1992. "Domain Wall Motion in Piezoelectric Materials under High Stress," In: *Proceedings of the Eighth IEEE International on the Applications of Ferroelectrics (ISAF '92)*, IEEE, pp. 167–170.
- Strukov, B.A. and Levanyuk, A.P. 1998. *Ferroelectric Phenomena in Crystals - Physical Foundations*, Springer, Germany.
- Takase, S. 1999. "Piezoelectric Actuator and Fuel-injection Apparatus using the Actuator," United States Patent, Patent Number 6-155-500.
- Uchino, K. and Hirose, S. 2001. "Loss Mechanisms in Piezoelectrics: How to Measure Different Losses Separately," *IEEE Transactions on Ultrasonics, Ferroelectrics, and Frequency Control*, 48(1):307–312.
- Yao, K., Uchino, K., Xu, Y., Dong, S. and Lim, L.C. 2000. "Compact Piezoelectric Stacked Actuators for High Power Applications," *IEEE Transactions on Ultrasonics and Frequency Control*, 47(4):819–825.
- Zhang, Q.M., Wang, H., Kim, N. and Cross, L.E. 1994. "Direct Evaluation of Domain-wall and Intrinsic Contributions to the Dielectric and Piezoelectric Response and their Temperature Dependence on Lead Zirconate Titanate Ceramics," *Journal of Applied Physics*, 75(1):454–459.
- Zhang, Q.M., Wang, H. and Zhao, J. 1995. "Effect of Driving Field and Temperature on the Response Behavior of Ferroelectric Actuator and Sensor Materials," *Journal of Intelligent Material Systems and Structures*, 16:84–93.
- Zheng, J., Takahashi, S., Yokikawa, S., Uchino, K. and de Vries, J.W.C. 1996. "Heat Generation in Multilayer Piezoelectric Actuators," *Journal of American Ceramics Society*, 79(12): 3193–3198.